Thermal Analysis of Lateral-Current-Injection Membrane Distributed Feedback Laser

Kyohei Doi, Takahiko Shindo, *Member, IEEE*, Jieun Lee, Tomohiro Amemiya, *Member, IEEE*, Nobuhiko Nishiyama, *Senior Member, IEEE*, and Shigehisa Arai, *Fellow, IEEE*

***Abstract*— We theoretically investigated the self-heating effect caused by current injection into a membrane distributed feedback laser designed to operate at ultralow-power consumption. By simulating its temperature distribution, the thermal resistance of the laser was estimated to be 6100 K/W. In addition, changes in lasing characteristics owing to the self-heating effect were calculated. An output power of 0.18 mW—which is adequate for an on-chip light source—can be obtained at a driving power of 1 mW. We proved that, owing to its ultralow-threshold operation, the self-heating effect has little effect on the lasing characteristics of the membrane laser.**

***Index Terms*— DFB laser, membrane laser, optical interconnection, semiconductor laser, strong optical confinement, thermal analysis, thermal resistance.**

I. Introduction

LARGE scale integrated circuits (LSIs) face considerable performance limitations caused by factors such as resistive capacitive (RC) delays and large transmission losses in their electrical global wiring [1], [2]. One promising method for solving this problem is the use of optical interconnections [3]–[5]. For on-chip optical interconnection, a light source (e.g., a directly modulated semiconductor laser or external optical modulator) operating at less than 100 fJ/bit is required [6]; this corresponds to a driving power of 1 mW at a modulation speed of 10 Gb/s. By assuming that the minimum receivable power of a pin photodiode has a typical value of −13 dBm (0.05 mW at a bit-error-rate of 10^{-9} at 10 Gb/s) and that the total loss between the light source and photodiode (which also includes the quantum efficiency of the photodiode) is 5dB, the required output of the light source becomes −8 dBm (0.16 mW); as such, a light source with ultra-low power-consumption and high-speed (>10 Gb/s) operational capability is required to successfully achieve on-chip optical interconnection. Owing to their strong ability to be optically confined within very small cavities, vertical cavity surface emitting lasers (VCSELs) [7]–[11] and microdisk lasers [12], [13] have shown promise in this respect, and in recent years extremely low-power operation and high-speed transmission using micro cavity photonic crystal (PhC) lasers and photodiodes has been demonstrated [14]–[18].

As an alternative, the authors have proposed and demonstrated a semiconductor membrane distributed feedback (DFB) laser containing a thin (150–200 nm) semiconductor core layer sandwiched between low-refractive index cladding layers composed of SiO_2, BCB, and air. Because of the strong optical confinement effect of the semiconductor membrane structure caused by the large refractive index difference between the core and cladding layers, ultra-low-threshold operation could be confirmed experimentally through optical pumping [19]–[21]. In order to electrically pump a membrane laser, a lateral-current-injection (LCI) scheme [22] can be adopted and, using a surface grating structure, an electrically pumped LCI membrane DFB laser was demonstrated [23]–[27].

Because of its ultra-low power-consumption and ability to integrate more fully with in-plane photonic devices, the membrane laser is one of more promising technologies for achieving on-chip optical interconnection; however, owing to the low thermal conductivity of the semiconductor membrane structure itself, there remain concerns about self-heating from current injection.

In this study, we conducted a thermal analysis of the semiconductor membrane laser in order to better understand the self-heating effect. In Section II, the temperature distribution and thermal resistance of the semiconductor membrane laser are numerically analyzed. In Section III, the self-heating effect is used to develop a simulation of the light output characteristics of the semiconductor membrane laser under both pulsed and continuous-wave (CW) conditions. Even though the thermal resistance of the semiconductor membrane laser is shown to be two orders of magnitude larger than that of a conventional (vertical current injection type) semiconductor laser, owing to its low operational current the self-heating induced temperature rise is found to be only a few degrees at close to room temperature.

II. Thermal Resistance of Membrane Laser

Fig. 1 shows a schematic device structure of a GaInAsP/InP membrane DFB laser with a surface grating on top of

Manuscript received November 15, 2013; revised February 19, 2014; accepted February 26, 2014. Date of publication March 5, 2014; date of current version March 19, 2014. This work was supported in part by the JSPS KAKENHI under Grants 24246061, 24656046, 25709026, 21226010, 25420321, and 13J08092, and in part by the Council for Science and Technology Policy through the FIRST Program.

K. Doi, T. Shindo, J. Lee, and N. Nishiyama are with the Department of Electrical and Electronic Engineering, Tokyo Institute of Technology, Tokyo 152-8552, Japan (e-mail: doi.k.ac@m.titech.ac.jp; shindou.t.aa@m.titech.ac.jp; lee.j.aj@m.titech.ac.jp).

T. Amemiya is with the Quantum Nanoelectronics Research Center, Tokyo Institute of Technology, Tokyo 152-8552, Japan (e-mail: amemiya.t.ab@m.titech.ac.jp).

S. Arai is with the Department of Electrical and Electronic Engineering, Tokyo Institute of Technology, Tokyo 152-8552, Japan, and also with the Quantum Nanoelectronics Research Center, Tokyo Institute of Technology, Tokyo 152-8552, Japan (e-mail: aria@pe.titech.ac.jp).

Color versions of one or more of the figures in this paper are available online at http://ieeexplore.ieee.org.

Digital Object Identifier 10.1109/JQE.2014.2309700

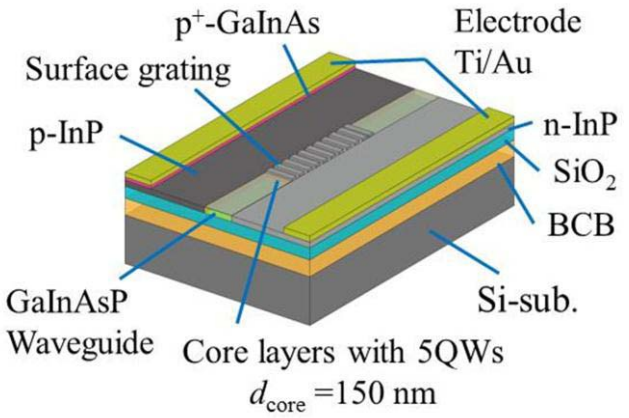

Fig. 1. Schematic device structure of a GaInAsP/InP membrane DFB laser with surface grating structure.

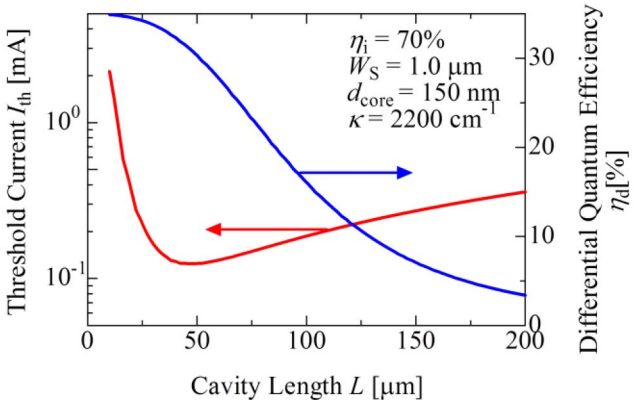

Fig. 2. Calculated threshold current and differential quantum efficiency per facet as a function of a cavity length.

TABLE I
THERMAL CONDUCTIVITY USED IN THE 2D FEM SIMULATION

Material	Thermal conductivity [W/K·m]
Cu	400
Au	320
Si	158
InP	68
$G_{0.22}In_{0.78}As_{0.81}P_{0.19}$ (well)	5.1
$G_{0.26}In_{0.74}As_{0.49}P_{0.51}$ (barrier)	5.2
$Ga_{0.47}In_{0.53}As$ (contact layer)	4.4
SiO_2	1.4
BCB	0.29

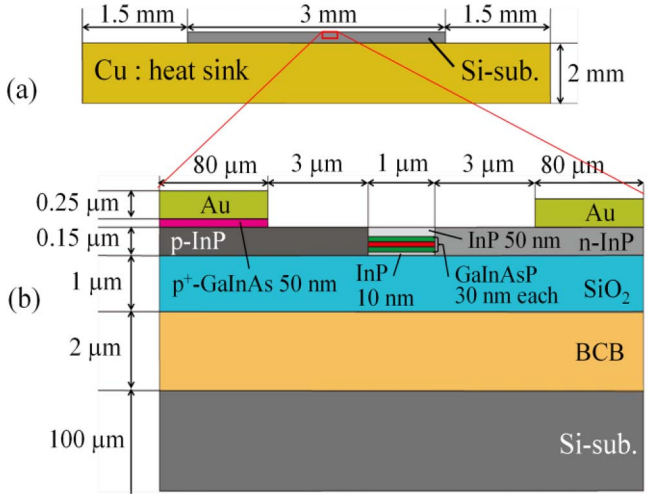

Fig. 3. (a) Overview of the simulation model and (b) detailed drawing of active layer surroundings.

the laser stripe. The core layer of the device consists of 5-quantum-wells (CS-5QWs, 6 nm-thick) that are 1% compressively strained and sandwiched above and below, respectively, by 50 and 10-nm-thick InP passivation layers. The top and bottom cladding layers consist, respectively of air (refractive index $n = 1$) and SiO_2 ($n = 1.45$). In order to enable the lateral injection of current, n-InP and p-InP inclusions have been formed on opposite sides of the core layer through a two-step regrowth process. The estimated optical confinement factor within the core layer structure is 3.8%/well.

Fig. 2 shows the calculated threshold current I_{th} and the external differential quantum efficiency η_d as a function of cavity length at an assumed surface grating depth of 30 nm, which corresponds to an index-coupling coefficient of 2200 cm^{-1}. As can be seen, the estimated minimum threshold current and external differential quantum efficiency are 0.12 mA and 31%/facet, respectively, at a cavity length of 48 μm; this suggests that the membrane laser should be able to operate at an ultra-low threshold current.

Next, we simulated the temperature distribution in the active layer of the membrane laser using a two dimensional model implemented with the finite element method (FEM), as shown in Fig. 3. In the model, the 5QWs were replaced by a bulk structure ($Ga_{0.26}In_{0.74}As_{0.49}P_{0.51}$ (30 nm), $Ga_{0.22}In_{0.78}As_{0.81}P_{0.19}$ (30 nm), $Ga_{0.26}In_{0.74}As_{0.49}P_{0.51}$ (30 nm)), and the simulation was based on the typical steady-state heat transfer equation [28]:

$$-\nabla \cdot (\kappa \nabla T) = Q \tag{1}$$

where Q is the heat source density, κ is the thermal conductivity, and T is the temperature. The thermal conductivities of the materials used in the simulation were obtained from previous reports [29] and [30] and are listed in Table I. The boundary conditions were given by:

$$T|_{\text{sink}} = T_s = 293[\text{K}], \tag{2}$$

$$\kappa \nabla T = h\,(T - T_s), \tag{3}$$

where T_s is the temperature at the bottom of the heat sink, and h is the heat transfer coefficient used to express heat flux to the air surrounding the laser bar and heat sink; these were assumed to be 293 K and 4.6 W/K·m^2, respectively. As an internal boundary condition, a thermal resistance equivalent to that of a 2-μm-thick air gap was assumed between the Si substrate and the heat sink; this was justified by the non-ideal heat transfer characteristics owing to the roughness of the contact interface.

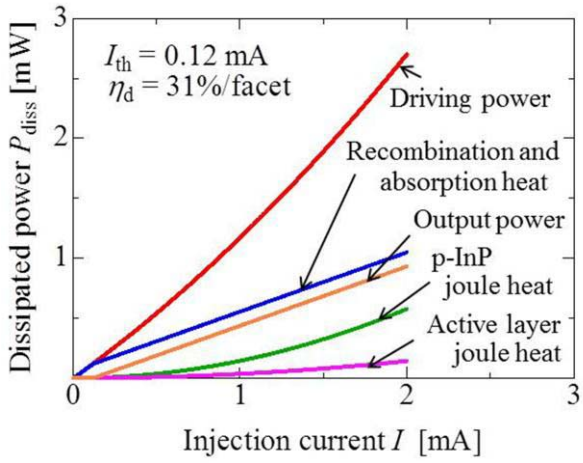

Fig. 4. Theoretical predictions of dissipated power as a function of injection current.

In the active region, values of the optical absorption, nonradiative recombination, and joule heat were all given with respect to the heat sources. In the part of the p-InP layer the current flows through, which is 6 μm from the stripe edge, joule heating owing to sheet resistance was assumed, while in the n-InP layer it was assumed to be negligible because the sheet resistance of the p-InP layer dominates the total series resistance of the LCI structure. Dissipated power P_{diss} is plotted as a function of the injection current of various laser sections in Fig. 4, which is expressed as follows:

$$\begin{aligned} P_{\mathrm{diss}} &= U_{\mathrm{act}} + P_{\mathrm{Joule,act}} + P_{\mathrm{Joule,p-InP}} \\ &= \left\{V_{\mathrm{d}} I - 2E_{\mathrm{g}}\eta_{\mathrm{d}}\left(I - I_{\mathrm{th}}\right)\right\} + R_{\mathrm{act}} I^2 + R_{\mathrm{p-InP}} I^2 \end{aligned} \quad (4)$$

where U_{act}, $P_{\mathrm{Joule,act}}$, $P_{\mathrm{Joule,p-InP}}$, V_{d}, I and E_{g} are, respectively, the total of optical absorption and nonradiative recombination heat, the joule heat in the active layer, the joule heat in the p-InP layer, the voltage drop across the active region, the bias current and the bandgap of 0.8 eV. When the driving power and corresponding driving current are 1 mW and 0.87 mA, respectively, the active and p-InP layers dissipated heat at $U_{\mathrm{act}} + P_{\mathrm{Joule,act}} = 0.52$ and $P_{\mathrm{Joule,p-InP}} = 0.11$ mW, respectively, at electric resistances of $R_{\mathrm{act}} = 35$ and $R_{\mathrm{p-InP}} = 145\ \Omega$, respectively.

Figs. 5 and 6 show the temperature distribution and heat flux distribution around the core layer of the membrane laser at a dissipated power P_{diss} of 0.63 mW. In Fig. 5 it can be seen that the maximum temperature and the temperature rise ΔT in the active layer are 296.8 and 3.8 K, respectively, at a membrane laser thermal resistance, R_{th} of 6100 K/W, which was calculated as follows:

$$R_{\mathrm{th}} = \frac{\Delta T}{P_{\mathrm{diss}}}. \quad (5)$$

This value is very high compared with the thermal resistance of conventional vertical-current-injection-type semiconductor lasers operating at 20–50 K/W [31]. As shown in Fig. 6, most of the heat generated in the active and p-InP layers flows laterally through the electrodes (Au) and through the InP because the thermal conductivities of the cladding air and

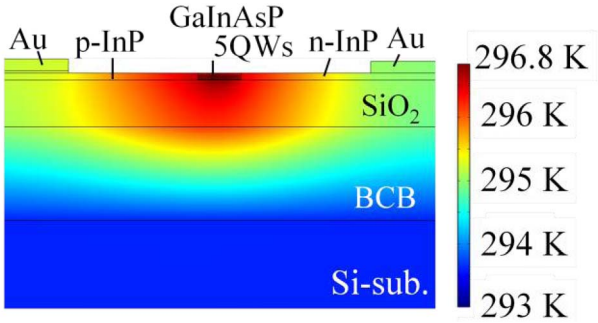

Fig. 5. Simulated two-dimensional temperature distribution in the membrane laser at a driving power of 1 mW (dissipated power P_{diss} of 0.63 mW).

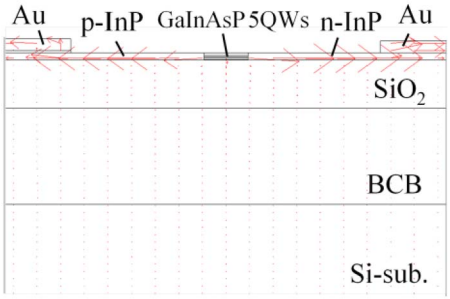

Fig. 6. Simulated two dimensional heat flux distribution in membrane laser at a driving power of 1 mW (dissipated power P_{diss} of 0.63 mW).

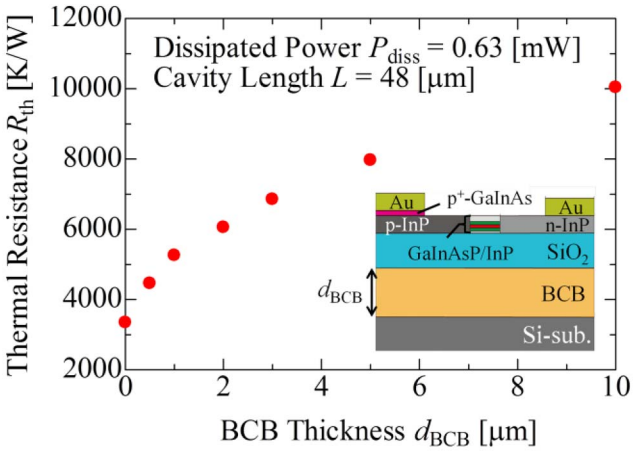

Fig. 7. Thermal resistance of membrane laser as a function of BCB thickness.

SiO_2 layers and the BCB adhesive layer are much lower than those of the electrodes and the InP layers.

Figs. 7 and 8 show thermal resistance as a function of BCB and Au thickness, respectively. As the BCB thins or the Au thickens, the thermal resistance decreases, which leads to decreased temperature rise in the active layer. This suggests that, thermal resistance can be reduced by making the Au thicker than 1 μm while ensuring that the BCB layer is as thin as possible; because SiO_2 act as a cladding layer in the structure, the thickness of the BCB can be reduced as long as bonding is possible.

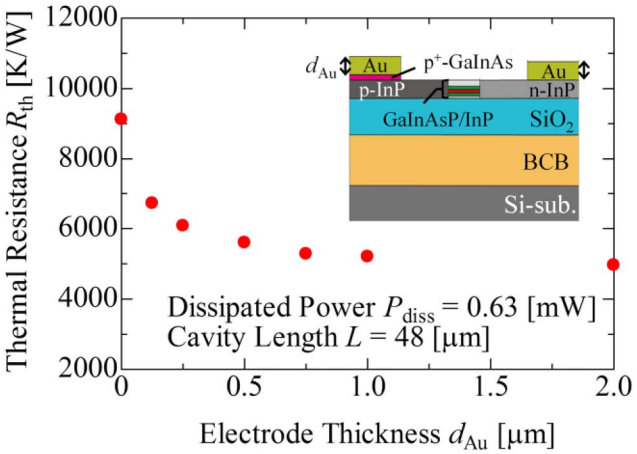

Fig. 8. Thermal resistance of membrane laser as a function of Au thickness.

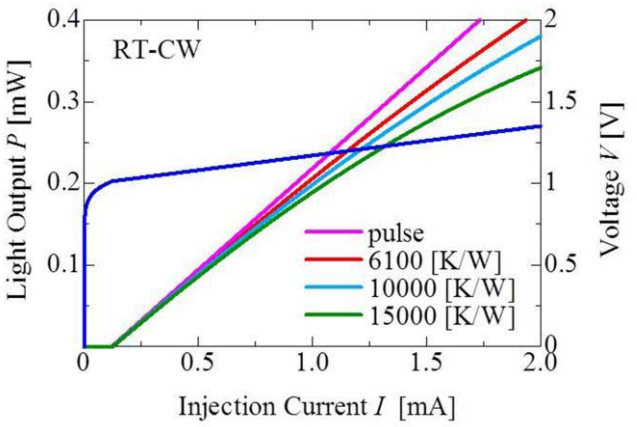

Fig. 9. Simulated light output power and voltage characteristics as a function of injection current at room temperature for various thermal resistances.

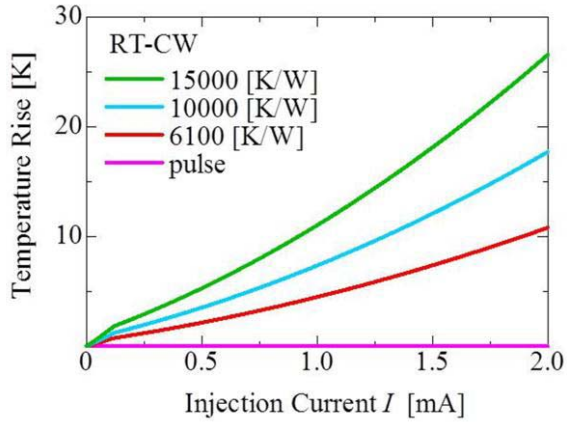

Fig. 10. Calculated temperature rise in the active region as a function of injection current for various thermal resistances.

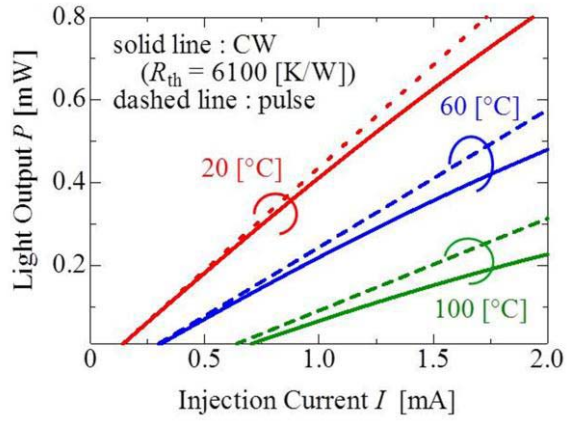

Fig. 11. Light output from both facets as a function of injection current at differing heat-sink temperatures of 20 °C, 60 °C, and 100 °C.

III. Simulated Lasing Characteristics

Using the thermal resistances derived in the previous section, simulations of the lasing characteristics of the membrane laser under CW conditions were conducted. The temperature dependencies of the threshold current and external differential quantum efficiency can be characterized by the respective characteristic temperatures T_0 and T_1 and expressed as follows:

$$I_{\text{th}}(T) = I_{\text{th}}(T_s) \exp\left(\frac{\Delta T}{T_0}\right), \tag{6}$$

$$\eta_{\text{d}}(T) = \eta_{\text{d}}(T_s) \exp\left(-\frac{\Delta T}{T_1}\right). \tag{7}$$

In 1.55 μm GaInAsP/InP double-heterostructure (DH) and quantum-well (QW) lasers, T_0 and T_1 are assumed to take the typical values of 50 and 100 K, respectively. The output power can then be expressed as [32]:

$$P_{\text{out}} = \eta_{\text{d}}(T)\, E_{\text{g}} \{I - I_{\text{th}}(T)\}. \tag{8}$$

Fig. 9 shows the lasing characteristics at various thermal resistances as a function of the injection current. The parameters used for this calculation are: $I_{\text{th}}(T_{\text{s}}) = 0.12$ mA; $\eta_{\text{d}}(T_{\text{s}}) = 31\%$/facet; and $E_{\text{g}} = 0.8$ eV. As can be seen, very little saturation of output power occurs from self-heating. At $R_{\text{th}} = 6100$ K/W, the output power is 0.18 mW, which represents an adequate output power of more than -8 dBm for an on-chip light source with a driving power and corresponding driving current of 1 mW and 0.87 mA, respectively.

Fig. 10 shows the temperature rise in the active layer as a function of the magnitude of injection current. As can be seen, the temperature rise ($\Delta T = R_{\text{th}} \times P_{\text{diss}}$, from Eq. (5)) in the active layer is only 3.8 K at a driving power of 1 mW; this value is quite low because the value of P_{diss} is low enough to compensate for the high thermal resistance of the membrane laser. These calculations analytically demonstrate the robustness of the lasing characteristics of the membrane laser; although its expected thermal resistance is very high, its ultra-low-power-consumption operation diminishes self-heating caused by current injection.

As Fig. 9 shows a DFB structure with a uniform grating lacking a phase shift region, the light output by one side is equal to half of the total output. However, a more unbalanced directional output is required for membrane lasers used in photonic integrated circuits; this can be achieved by adopting an asymmetric grating with a phase shift region or

a distributed reflector (DR) structure [33], [34]. Calculated total output power dependencies on injection current at heat-sink temperatures of 20, 60, and 100 °C are shown in Fig. 11, in which the solid lines indicate the light output properties under CW conditions at a thermal resistance R_{th} of 6100 K/W, while the dashed lines indicate the output properties under pulsed conditions. At heat-sink temperatures of 20, 60, and 100 °C and an output power of −8 dBm (0.16 mW), the required operating current under CW conditions is higher than under pulsed conditions by 3, 6, and 18%, respectively, while the temperature rises ΔT are 2.0 (20°), 4.6 K (60°) and 12 K (100 °C), respectively. From these calculations, it can be seen that the output power does not effectively saturate from current injection-induced self-heating at heat-sink temperatures below 100 °C, even though the thermal resistance of the membrane laser is very high. Although the model was not able to achieve the adequate output power of −8 dBm (0.16 mW) at a heat-sink temperature and driving power of 100 °C and 1 mW, respectively, owing to the high threshold current and low external differential quantum efficiency at such high heat-sink temperature, this effect was not caused by the self-heating effect. To solve this problem, the use of Bragg wavelength detuning [35], [36] in an AlGaInAs/InP alloy system [37], [38] can effectively decrease the threshold current while increasing the external differential quantum efficiency at high heat-sink temperatures.

IV. Conclusion

In this study, we conducted a thermal analysis of self-heating caused by current injection in membrane DFB lasers. Using 2D FEM analysis, the thermal resistance was estimated to be 6100K/W, and the light output-voltage-current (L-V-I) properties were calculated under CW conditions at temperatures from 20 to 100 °C. Our results indicate that, in spite of its high thermal resistance, self-heating has a very small effect on the lasing characteristics of a membrane DFB laser owing to its ultra-low-threshold operation.

Acknowledgment

We thank Professors M. Asada, Y. Miyamoto, F. Koyama, S. Akiba, and T. Mizumoto, and Associate Professor M. Watanabe of the Tokyo Institute of Technology for the fruitful discussions.

References

[1] P. Kapur, J. P. McVittie, and K. C. Saraswat, "Technology and reliability constrained future copper interconnects-Part I: Resistance modeling," *IEEE Trans. Electron Devices*, vol. 49, no. 4, pp. 590–597, Apr. 2002.

[2] P. Kapur, G. Chandra, J. P. McVittie, and K. C. Saraswat, "Technology and reliability constrained future copper interconnects-Part II: Performance implications," *IEEE Trans. Electron Devices*, vol. 49, no. 4, pp. 598–604, Apr. 2002.

[3] D. A. B. Miller, "Rationale and challenges for optical interconnects to electronic chips," *Proc. IEEE*, vol. 88, no. 6, pp. 728–749, Jun. 2000.

[4] G. Chen *et al.*, "Prediction of CMOS compatible on-chip optical interconnect," *Integr., VLSI J.*, vol. 40, no. 4, pp. 434–446, Oct. 2006.

[5] K. Ohashi *et al.*, "On-chip optical interconnect," *Proc. IEEE*, vol. 97, no. 7, pp. 1186–1198, Jul. 2009.

[6] D. A. B. Miller, "Device requirements of optical interconnects to silicon chips," *Proc. IEEE*, vol. 97, no. 7, pp. 1166–1185, Jul. 2009.

[7] P. Moser *et al.*, "81 fJ/bit energy-to-data ratio of 850 nm vertical-cavity surface emitting lasers for optical interconnects," *Appl. Phys. Lett.*, vol. 98, no. 23, pp. 231106-1–231106-3, Jun. 2011.

[8] S. Imai *et al.*, "Recorded low power dissipation in highly reliable 1060-nm VCSELs for 'Green' optical interconnection," *IEEE J. Sel. Topics Quantum Electron.*, vol. 17, no. 6, pp. 1614–1620, Nov./Dec. 2011.

[9] A. Kasukawa, "VCSEL technology for green optical interconnects," *IEEE Photon. J.*, vol. 4, no. 2, pp. 642–646, Apr. 2012.

[10] M. P. Tan, A. M. Kasten, J. D. Sulkin, and K. D. Choquette, "Planar photonic crystal vertical-cavity surface-emitting lasers," *IEEE J. Sel. Topics Quantum Electron.*, vol. 19, no. 4, p. 4900107, Jul./Aug. 2013.

[11] Y. Rao *et al.*, "Long-wavelength VCSEL using high contrast grating," *IEEE J. Sel. Topics Quantum Electron.*, vol. 19, no. 4, p. 1701311, Jul./Aug. 2013.

[12] M. Fujita, R. Ushigome, and T. Baba, "Continuous wave lasing in GaInAsP microdisk injection laser with threshold current of 40 μA," *Electron. Lett.*, vol. 36, no. 9, pp. 790–791, Apr. 2000.

[13] J. V. Campenhout *et al.*, "Electrically pumped InP-based microdisk lasers integrated with nanophotonic silicon-on-insulator waveguide circuit," *Opt. Exp.*, vol. 15, no. 11, pp. 6744–6749, May 2007.

[14] S. Matsuo *et al.*, "High-speed ultracompact buried heterostructure photonic-crystal laser with 13 fJ of energy consumed per bit transmitted," *Nature Photon.*, vol. 4, no. 9, pp. 648–654, Sep. 2010.

[15] S. Matsuo *et al.*, "Room-temperature continuous-wave operation of lateral current injection wavelength-scale embedded active-region photonic-crystal laser," *Opt. Exp.*, vol. 19, no. 3, pp. 2242–2250, Jan. 2011.

[16] B. Ellis *et al.*, "Ultralow-threshold electrically pumped quantum-dot photonic-crystal nanocavity laser," *Nature Photonics*, vol. 5, no. 5, pp. 297–300, May 2011.

[17] S. Matsuo *et al.*, "20-Gbit/s directly modulated photonic crystal nanocavity laser with ultra-low power consumption," *Opt. Exp.*, vol. 20, no. 4, pp. 3773–3780, Jan. 2012.

[18] T. Sato *et al.*, "Ultra-low threshold current CW operation of photonic crystal nanocavity laser with InAlAs sacrificial layer," in *Proc. 23rd IEEE Int. Semicond. Laser Conf. (ISLC)*, San Diego, CA, USA, Oct. 2012, pp. 169–170.

[19] T. Okamoto, N. Nunoya, Y. Onodera, T. Yamazaki, S. Tamura, and S. Arai, "Optically pumped membrane BH-DFB lasers for low-threshold and single-mode operation," *IEEE J. Sel. Topics Quantum Electron.*, vol. 9, no. 5, pp. 1361–1366, Sep./Oct. 2003.

[20] S. Sakamoto *et al.*, "Strongly index-coupled membrane BH-DFB lasers with surface corrugation grating," *IEEE J. Sel. Topics Quantum Electron.*, vol. 13, no. 5, pp. 1135–1141, Sep./Oct. 2007.

[21] S. Sakamoto *et al.*, "85 °C continuous-wave operation of GaInAsP/InP-membrane buried heterostructure distributed feedback lasers with polymer cladding layer," *Jpn. J. Appl. Phys.*, vol. 46, no. 47, pp. L1155–L1157, Nov. 2007.

[22] K. Oe, Y. Noguchi, and C. Caneau, "GaInAsP lateral current injection lasers on semi-insulating substrates," *IEEE Photon. Technol. Lett.*, vol. 6, no. 4, pp. 479–481, Apr. 1994.

[23] T. Shindo *et al.*, "GaInAsP/InP lateral-current-injection distributed feedback laser with a-Si surface grating," *Opt. Exp.*, vol. 19, no. 3, pp. 1884–1891, Jan. 2011.

[24] T. Shindo *et al.*, "Lasing operation of lateral-current-injection membrane DFB laser with surface grating," in *Proc. 16th Opto-Electron. Commun. Conf. (OECC)*, Kaohsiung, Taiwan, Jul. 2011, pp. 287–288.

[25] T. Shindo *et al.*, "Lateral-current-injection distributed feedback laser with surface grating structure," *IEEE J. Sel. Topics Quantum Electron.*, vol. 17, no. 5, pp. 1175–1182, Sep./Oct. 2011.

[26] S. Arai, N. Nishiyama, T. Maruyama, and T. Okumura, "GaInAsP/InP membrane lasers for optical interconnects," *IEEE J. Sel. Topics Quantum Electron.*, vol. 17, no. 5, pp. 1381–1389, Sep./Oct. 2011.

[27] M. Futami, T. Shindo, K. Doi, T. Amemiya, N. Nishiyama, and S. Arai, "Low-threshold operation of LCI-membrane-DFB lasers with Be-doped GaInAs contact layer," in *Proc. 24th Int. Conf. Indium Phosphide Rel. Mater. (IPRM)*, Santa Barbara, CA, USA, Aug. 2012, pp. 285–288, paper Th-2C.5.

[28] H. K. Lee, Y. M. Song, Y. T. Lee, and J. S. Yu, "Thermal analysis of asymmetric intracavity-contracted oxide-aperture VCSELs for efficient heat dissipation," *Solid State Electron.*, vol. 53, no. 10, pp. 1086–1091, Jun. 2009.

[29] W. Nakwaski, "Thermal conductivity of binary, ternary, and quaternary III-V compounds," *J. Appl. Phys.*, vol. 64, no. 1, pp. 159–166, Jul. 1988.

[30] G. Hatakoshi, M. Onomura, M. Yamamoto, S. Nunoue, K. Itaya, and M. Ishikawa, "Thermal analysis for GaN laser diodes," *Jpn. J. Appl. Phys.*, vol. 38, no. 5A, pp. 2764–2768, May 1999.
[31] W. B. Joyce and R. W. Dixon, "Thermal resistance of heterostructure lasers," *J. Appl. Phys.*, vol. 46, no. 2, pp. 855–862, Feb. 1975.
[32] M. N. Sysak *et al.*, "Experimental and theoretical thermal analysis of a hybrid silicon evanescent laser," *Opt. Exp.*, vol. 15, no. 23, pp. 15041–15046, Oct. 2007.
[33] J. I. Shim, K. Komori, S. Arai, I. Arima, and Y. Suematsu, "Lasing characteristics of 1.5-μm GaInAsP/InP SCH-BIG-DR lasers," *IEEE J. Quantum Electron.*, vol. 27, no. 6, pp. 1736–1745, Jun. 1991.
[34] K. Ohira, T. Murayama, S. Tamura, and S. Arai, "Low-threshold and high-efficiency operation of distributed reflector lasers with width-modulated wirelike active regions," *IEEE J. Sel. Topics Quantum Electron.*, vol. 11, no. 5, pp. 1162–1168, Sep./Oct. 2005.
[35] H. Lu, C. Blaauw, and T. Makino, "Single-mode operation over a wide temperature range in 1.3 μm InGaAsP/InP distributed feedback lasers," *IEEE J. Lightw. Technol.*, vol. 14, no. 5, pp. 851–859, May 1996.
[36] Y. Nishimoto *et al.*, "High T_0 operation of 1590 nm GaInAsP/InP quantum-wire distributed feedback lasers by Bragg wavelength detuning," *Jpn. J. Appl. Phys.*, vol. 46, no. 17, pp. L411–L413, May 2007.
[37] C. E. Zah *et al.*, "High-performance uncooled 1.3-μm $Al_xGayIn_{1-x-y}As$/InP strained-layer quantum-well lasers for subscriber loop applications," *IEEE J. Quantum Electron.*, vol. 30, no. 2, pp. 511–523, Feb. 1994.
[38] Y. Takino, M. Shirao, T. Sato, N. Nishiyama, T. Amemiya, and S. Arai, "Regrowth interface quality dependence on thermal cleaning of AlGaInAs/InP buried-heterostructure lasers," *Jpn. J. Appl. Phys.*, vol. 50, no. 7, pp. 070203-1–070203-3, Jul. 2011.

Kyohei Doi was born in Saitama, Japan, in 1988. He received the B.E. degree in electrical and electronic engineering from the Tokyo Institute of Technology, Tokyo, Japan, in 2012, where he is currently pursuing the M.E. degree in electrical and electronic engineering.

His current research interests include membrane-based photonic devices for optical interconnection.

Mr. Doi is a member of the Japan Society of Applied Physics.

Takahiko Shindo (S'10–M'12) received the B.E., M.E., and Ph.D. degrees in electrical and electronic engineering from the Tokyo Institute of Technology, Japan, in 2008, 2010, and 2012, respectively.

Since 2012, he has been working on semiconductor lasers with ultralow-power consumption operation as a Research Fellow with the Japan Society for the Promotion of Science, Japan, and has been with the NTT Photonics Laboratories since 2013.

Dr. Shindo is a member of the Japan Society of Applied Physics. He received the Best Student Paper Award at the Opto-Electronics and Communications Conference, Taiwan, in 2011, and the Ericsson Young Scientist Award in 2012.

Jieun Lee received the B.E. degree in electronics and radio engineering from Kyung Hee University, Korea, and the M.E. degree in electrical and electronic engineering from the Tokyo Institute of Technology, Japan, in 2009 and 2012, respectively, where she is currently pursuing the Ph.D. degree in electrical and electronic engineering.

Her current research interests include membrane-based photonic integrated devices for optical interconnection. She is a member of the Japan Society of Applied Physics.

Tomohiro Amemiya (S'06–M'09) received the B.S., M.S., and Ph.D. degrees in electronic engineering from the University of Tokyo, Japan, in 2004, 2006, and 2009, respectively.

In 2009, he was with the Quantum Electronics Research Center, Tokyo Institute of Technology, where he is currently an Assistant Professor. His research interests include the physics of semiconductor light-controlling devices, metamaterials for optical frequency, magnetooptical devices, and the processing technologies for fabricating these devices.

Dr. Amemiya is a member of the Optical Society of America, the American Physical Society, and the Japan Society of Applied Physics. He was the recipient of the 2007 IEEE Photonics Society Annual Student Paper Award and the 2008 IEEE Photonics Society Graduate Student Fellowship.

Nobuhiko Nishiyama (M'01–SM'07) was born in Yamaguchi, Japan, in 1974. He received the B.E., M.E., and Ph.D. degrees from the Tokyo Institute of Technology, in 1997, 1999, and 2001, respectively. During the Ph.D. work, he demonstrated single-mode 0.98- and 1.1-μm VCSEL arrays with stable polarization using misoriented substrates for high-speed optical networks as well as MOCVD-grown GaInNAs VCSELs. He was with Corning Incorporated, Corning, NY, USA, in 2001, and with the Semiconductor Technology Research Group. At Corning, he was involved in several subjects, including short-wavelength lasers, 1060-nm DFB/DBR lasers, and long-wavelength InP-based VCSELs. Since 2006, he has been an Associate Professor with the Tokyo Institute of Technology. His current main interests are focused on transistor lasers, silicon photonics, III-V silicon hybrid optical devices, and terahertz-optical signal conversions involving optics-electronics-radio integration circuits.

He received an Excellent Paper Award from the Institute of Electronics, Information, and Communication Engineers of Japan in 2001 and the Young Scientists Prize in the Commendation for Science and Technology from the Minister of Education, Culture, Sports, Science, and Technology in 2009.

Dr. Nishiyama is a member of the Japan Society of Applied Physics, the Institute of Electronics, Information, and Communication Engineers (IEICE), and the IEEE Photonics Society. He is currently appointed as the Chair of the technical group of silicon-photonics in IEICE.

Shigehisa Arai (M'83–SM'06–F'10) was born in Kanagawa, Japan, in 1953. He received the B.E., M.E., and D.E. degrees in electronics from the Tokyo Institute of Technology, Japan, in 1977, 1979, and 1982, respectively. During the Ph.D. work, he demonstrated room-temperature CW operations of 1.11–1.67-μm long-wavelength lasers fabricated by liquid-phase epitaxy as well as their single-mode operations under rapid direct modulation.

He was with the Department of Physical Electronics, Tokyo Institute of Technology, as a Research Associate in 1982, and with the AT&T Bell Laboratories, Holmdel, NJ, USA, as a Visiting Researcher from 1983 to 1984, on leave from the Tokyo Institute of Technology. Then he became a Lecturer in 1984, an Associate Professor in 1987, and a Professor with the Research Center for Quantum Effect Electronics and the Department of Electrical and Electronic Engineering in 1994. Since 2004, he has been a Professor with the Quantum Nanoelectronics Research Center, Tokyo Institute of Technology. His research interests include photonic integrated devices, such as dynamic-single-mode and wavelength-tunable semiconductor lasers, semiconductor optical ampli?ers, and optical switches/modulators. His current research interests include studies of low-damage and cost-effective processing technologies of ultra?ne structures for high-performance lasers and photonic integrated circuits on silicon platforms.

Dr. Arai is a member of the Optical Society of America, a fellow of the Institute of Electronics, Information, and Communication Engineers (IEICE), and the Japan Society of Applied Physics. He received an Excellent Paper Award from the IEICE of Japan in 1988, the Michael Lunn Memorial Award from the Indium Phosphide and Related Materials Conference in 2000, the Prizes for Science and Technology, including a Commendation for Science and Technology from the Minister of Education, Culture, Sports, Science, and Technology in 2008, an Electronics Society Award in 2008, and the Achievement Award from the IEICE in 2011.